Theoretical Investigation of the Role of Intramolecular Hydrogen Bonding in β-Hydroxyethoxy and β-Hydroxyethylperoxy Radicals in the Tropospheric Oxidation of Ethene

Luc Vereecken and Jozef Peeters*

Department of Chemistry, University of Leuven, Celestijnenlaan 200F, B-3001, Leuven, Belgium

Received: June 18, 1998; In Final Form: January 14, 1999

In this work, we performed a quantum chemical B3LYP-DFT/6-31G** characterization of the geometries, vibrational frequencies, and relative energies of the various internal-rotation conformers of the title radicals and of the transition structures for the $HOCH_2CH_2O \rightarrow CH_2OH + CH_2O$ dissociation, thereby obtaining the first evidence for intramolecular hydrogen bonding in these molecules. For both the peroxy and oxy radicals, some of the equilibrium geometries were found to be stabilized by interactions between the hydroxy H and the (per)oxy O, lowering the energies by 1.5−2.5 kcal/mol, as confirmed by single point CCSD(T) calculations; it is concluded that thermalized populations at ambient temperatures should consist predominantly of the H-bonded rotamers. Furthermore, the hydrogen bond was found to persist in the transition state for dissociation of the H-bonded $HOCH_2CH_2O$ rotamers, resulting in an energy barrier calculated to be only 10 kcal/mol, in excellent accord with recent experimental results. Based on the DFT characterizations and using advanced statistical energy partitioning theories, a Master Equation analysis was performed predicting that at 298 K and 1 atm, 38% of the $HOCH_2CH_2O$ radicals formed in the atmospheric $HOCH_2CH_2OO + NO$ reaction dissociate "promptly" before collisional stabilization; also, the rate constant of the thermal dissociation of $HOCH_2CH_2O$ was theoretically evaluated at 2.1×10^5 s^{-1} at 298 K and 1 atm. These values, which are crucially dependent on the persistence of the H-bond during $HOCH_2CH_2O$ dissociation, likewise compare favorably with recent experimental data. Isomerization of $HOCH_2CH_2OO$ to OCH_2CH_2OOH was found to be of only minor importance to the oxidation of ethene. Theoretical results are also presented on the thermal dissociation of ethoxy and isopropoxy radicals.

Introduction

The oxidation of nonmethane hydrocarbons (NMHCs) is an important source of photochemical oxidants in the lower atmosphere. Ethene is among the more abundant NMHCs, emitted both by natural sources (vegetation, soils, and oceans) and by antropogenic sources (burning of biomass and of fossil fuels). In this work, we present an ab initio and theoretical-kinetics study of the β-hydroxyethylperoxy and β-hydroxyethoxy radicals involved in the OH-initiated tropospheric oxidation of ethene. This paper is complementary to the recent investigation by Orlando et al.[1] of the oxidation of ethene in atmospheric conditions.

The oxidation of ethene in the atmosphere is initiated predominantly by reaction with OH radicals, followed by reaction with O_2:[1−3]

$$OH + C_2H_4 + M \rightarrow HOCH_2CH_2 + M \quad (1)$$

$$HOCH_2CH_2 + O_2 \rightarrow HOCH_2CH_2OO \quad (2)$$

In the presence of NO_x, the resulting β-hydroxyethylperoxy radical can combine with NO to form a chemically activated peroxynitrite intermediate that dissociates promptly to NO_2 and a vibrationally excited hydroxyalkoxy radical:[1−3]

$$HOCH_2CH_2OO + NO \rightarrow HOC_2H_4OONO^{\dagger} \rightarrow NO_2 + HOCH_2CH_2O^{\dagger} \quad (3)$$

The overall exoergicity of the oxidation of NO by alkylperoxy radicals is usually in the 10−15 kcal/mol range.[3] The excited hydroxyethoxy radical either decomposes "promptly", by C−C bond rupture, or loses its excess energy in collisions with the bath gas:

$$HOCH_2CH_2O^{\dagger} \rightarrow CH_2OH + CH_2O \quad (4)$$

$$HOCH_2CH_2O^{\dagger} + M \rightarrow HOCH_2CHO + M \quad (5)$$

The relaxed oxy radicals then either decompose thermally, or react with oxygen molecules:

$$HOCH_2CH_2O + M \rightarrow CH_2OH + CH_2O + M \quad (6)$$

$$HOCH_2CH_2O + O_2 \rightarrow HOCH_2CHO + HO_2 \quad (7)$$

The relative importance of the oxidation products depends first on the ratio of the rates of prompt dissociation (4) and collisional stabilization (5), and second on the competition between thermal dissociation (6) and reaction with O_2 (7). Crucial to both ratios will be the height of the energy barrier to decomposition. The first ratio depends on total pressure but is only slightly influenced by temperature. The competition between reactions

* E-mail: Jozef.Peeters@chem.kuleuven.ac.be.

10.1021/jp9826930 CCC: $18.00
Published on Web 03/06/1999

6 and 7 is highly sensitive to temperature and can also depend on total pressure.

Both the hydroxyethylperoxy- and the hydroxyethoxy radicals of this mechanism can be stabilized by an intramolecular hydrogen bond between the hydrogen of the hydroxy function and an oxygen of the (per)oxy radical site. Similar internal H-bonding in β-hydroxyketones is well documented.[4] The aims of this theoretical work were to perform an ab initio characterization of the intramolecular hydrogen bonding in these radicals and to model the effects thereof on the kinetics of reactions 4−6. The H-bonding in the hydroxyethoxy radicals may be expected to increase the height of the energy barrier to the C−C scission and hence to slow the dissociation reactions 4 and 6.

Since the peroxy and oxy radicals have several degrees of freedom of internal rotation (three and two, respectively), these molecules exhibit extensive rotational conformerism. Using a suitable quantum chemical method, we identified and characterized all rotamers, with and without hydrogen bonds, to evaluate their relative stabilities and hence their contributions in both chemically activated and thermal populations. On the basis of these relative energies and vibrational data, we performed a theoretical analysis of the prompt formation of the dissociation products $CH_2OH + CH_2O$ by the reaction sequence (3) and (4), as well as of their formation from thermalized oxy radicals via reaction 6, permitting a comparison of theoretical predictions to the experimental data of Orlando et al.[1] A basic outline of the theoretical analysis and some final results were already presented together with those experimental data;[1] in the present paper we give a thorough description of the fundamentals and of the implementation.

Computational Details

The geometry optimizations and subsequent frequency calculations were performed at the B3LYP-DFT level of theory, i.e., Becke's three-parameter nonlocal-exchange functional[5] with the nonlocal correlation functional of Lee, Yang, and Parr.[6] The basis set used was 6-31G** for all calculations. The transition states were verified by IRC calculations at the same level of theory. The vibrational frequencies reported here have been systematically scaled by a factor of 0.9614, as reported by Scott and Radom[7] for the 6-31G* basis set. No significant spin contamination was found for the DFT wavefuctions (see Table 2); after annihilation of the first spin contaminant ⟨S**2⟩ becomes 0.7500 in all cases. The use of density functional theory as the prime tool of quantum chemical characterization warrants some justification and verification, as DFT sometimes fails (e.g., for hydrogen transfer reactions or strongly multireferenced systems). It is generally known that B3LYP-DFT geometries and vibrational frequencies correspond closely to experimental data. We have used B3LYP-DFT/6-31G** for calculation of transition state barrier heights on open shell species before,[8] obtaining excellent agreement with available literature data, and with high level single point CASPT2 calculations (average difference in relative energies for all saddlepoints on the C_3H_3 surface = 1.0 kcal/mol). Hobza et al.[9] found that B3LYP-DFT gives reliable results for H-bonded clusters. Regarding the decomposition of (hydroxy)alkoxy radicals, the available experimental data (although sparse) permits us to assess the accuracy of B3LYP-DFT/6-31G** for these systems in particular. Sample calculations (see Supporting Information) for the C−C scission of ethoxy gave a barrier height of 18.9 kcal/mol. Somnitz and Zellner[10] calculated a barrier height of 17.0 kcal/mol at the G2(MP2,SVP) level of theory (TS geometries optimized using QCI/6-31G*). Batt and Milne[11] measured a rate constant of 1.26×10^4 s^{-1} for this decomposition at 433.2 K and at ∼1 atm of CF_4, from which one can derive the barrier height value by standard transition state theory (see also below). Using our DFT rovibrational data, we find a preexponential factor of 3.17×10^{13} s^{-1}. This leads to a barrier value of 18.6 kcal/mol, assuming that the reaction rate is at its high-pressure limit. Devolder et al.[12] measured the isopropoxy dissociation rate constants directly over large pressure ranges for $T = 332-410$ K; by a Troe analysis of the falloff curves, they find the following high-pressure Arrhenius expression: $k_\infty = 5.1 \times 10^{13} \exp(-14.7 \text{ kcal·mol}^{-1}/RT)$ s^{-1}. This compares well with the B3LYP-DFT/6-31G** barrier height of 15.2 kcal/mol for the C−C bond scission in isopropoxy radicals (see Supporting Information) and the TST preexponential factor of 4.4×10^{13} s^{-1} at 370 K based on the DFT rovibrational data. For the decomposition of 2-butoxy to $CH_3CHO + C_2H_5$, Somnitz and Zellner[11] find a G2(MP2,SVP) barrier height of 11.5 kcal/mol, while Jungkamp et al.[13] found this transition state with B3LYP-DFT/6-31G** at 11.8 kcal/mol above the alkoxy radical. All this indicates that for these systems B3LYP-DFT/6-31G** results are close to higher level ab initio results and, more importantly, agree with experimental data within 0.5 kcal/mol. For the β-hydroxyethoxy decomposition itself, we can compare to the experimentally derived barrier height reported earlier.[1]

To verify the accuracy of the DFT relative energies for the different rotamers, we carried out single-point CCSD(T)/6-

TABLE 1: Zero-Point-Energy Corrected Relative Energies for All Rotamers of the β-Hydroxyethylperoxy Radicals and β-Hydroxyethoxy Radicals, the Transition States for C−C Bond Rupture in β-Hydroxyethoxy Radicals, and Its Reaction Products

structure[a]	dihedral angles (degrees) OCCO	HOCC	CCOO	ZPE (kcal/mol)	rel. energy (kcal/mol)
β-Hydroxyethylperoxy Radicals $HOCH_2CH_2OO$					
pmm	77.0	−51.1	−58.5	46.70	0.00
pmp	64.6	−64.1	71.9	46.51	1.13
pmt	66.1	−61.7	−170.5	46.42	1.79
ptp	70.5	−166.6	69.2	46.26	2.69
tpp	178.4	74.8	73.4	46.47	2.77
ttp	178.2	178.6	73.1	46.32	3.03
tpm	179.2	75.8	−73.0	46.44	3.05
ppp	63.8	67.7	69.8	46.36	3.22
ptt	73.4	−169.6	−178.8	46.13	3.44
ppt	65.9	64.5	−174.0	46.18	3.74
ttt (C_s)	180.0	180.0	180.0	46.16	3.94
tpt	177.9	73.2	176.6	46.26	3.98
ptm	72.6	−164.1	−98.7	46.13	3.99
ppm	∼65	∼65	∼−65	Rotamer not stable	
β-Hydroxyethoxy Radicals $HOCH_2CH_2O$					
pm	50.5	−45.7		43.23	0.00
tt (C_s)	180.0	180.0		42.30	1.86
tp	176.2	72.9		42.57	2.21
pt	72.8	−170.5		42.26	2.70
pp	68.9	66.6		42.67	3.34
Transition States for C−C Bond Rupture in $HOCH_2CH_2O$[b] Dissociation Products[b]					
TS_pm	47.9	−44.9		41.43	9.89
TS_tp	−172.4	81.4		41.14	11.82
TS_pp	69.1	78.8		41.07	13.15
$CH_2O\cdots HOCH_2$ (H-bonded complex)				40.56	5.03
$CH_2O + HOCH_2$ (infinite separation)				38.74	8.24[c]

[a] The name is based on the dihedral angles: "p" for dihedral angles of ∼+65°, "m" for ∼ −65°, and "t" for angles close to 180°. [b] Energies relative to $HOCH_2CH_2O$ rotamer pm. [c] Corrected for BSSE.

TABLE 2: Comparison of the B3LYP-DFT and CCSD(T) Energies for All Structures

	energy/hartree (⟨S**2⟩[a])		rel energy (kcal/mol)[b]	
structure	B3LYP-DFT	CCSD(T)	B3LYP-DFT	CCSD(T)
	β-Hydroxyethylperoxy Radicals $HOCH_2CH_2OO$			
pmm	−304.7466785 (0.7532)	−303.9553327 (0.7613)	−2.83	−2.32
pmp	−304.7445619 (0.7531)	−303.9542873 (0.7607)	−1.70	−1.87
pmt	−304.7433681 (0.7528)	−303.9527348 (0.7602)	−1.04	−0.98
ptp	−304.7416903 (0.7530)	−303.9514290 (0.7607)	−0.14	−0.32
tpp	−304.7418962 (0.7530)	−303.9514280 (0.7607)	−0.06	−0.10
ttp	−304.7412240 (0.7530)	−303.9512246 (0.7607)	0.21	−0.13
tpm	−304.7413987 (0.7530)	−303.9509513 (0.7606)	0.22	0.16
ppp	−304.7409966 (0.7530)	−303.9504241 (0.7606)	0.39	0.41
ptt	−304.7402807 (0.7528)	−303.9496556 (0.7603)	0.61	0.67
ppt	−304.7398981 (0.7528)	−303.9490295 (0.7603)	0.91	1.11
ttt (C_s)	−304.7395408 (0.7528)	−303.9492490 (0.7602)	1.11	0.95
tpt	−304.7396243 (0.7528)	−303.9489831 (0.7602)	1.15	1.22
ptm	−304.7393983 (0.7530)	−303.9487943 (0.7605)	1.16	1.20
	β-Hydroxyethoxy Radicals $HOCH_2CH_2O$			
pm	−229.5841892 (0.7532)	−228.9753877 (0.7584)	−2.02	−1.81
tt (C_s)	−229.5797539 (0.7531)	−228.9713955 (0.7581)	−0.16	−0.23
tp	−229.5796258 (0.7531)	−228.9710341 (0.7580)	0.18	0.26
pt	−229.5783462 (0.7529)	−228.9702465 (0.7583)	0.68	0.44
pp	−229.5779736 (0.7531)	−228.9694793 (0.7583)	1.32	1.34
	Transition states for C−C bond rupture in $HOCH_2CH_2O$, and dissociation products			
TS_pm	−229.5655539 (0.7601)	−228.9495797 (0.8871)	7.87	12.59
TS_tp	−229.5620251 (0.7625)	−228.9470874 (0.9057)	9.80	13.86
TS_pp	−229.5597969 (0.7628)	−228.9442160 (0.9175)	11.13	15.59
$CH_2O\cdots HOCH_2$	−229.5719329 (0.7531)	−228.9644378 (0.7601)	3.01	2.40
$CH_2O + HOCH_2$	−229.5596161 (0.7529)	−228.9522367 (0.7599)	6.22[c]	5.01[c]

[a] Spin operator expectation value for the DFT and UHF wave functions before annihilation of the first contaminant. For the separated products, the value for CH_2OH is reported. [b] The average energy of the rotamers is taken as zero. For the transition states and products, the same zero as for the $HOCH_2CH_2O$ rotamers is used. All relative energies are corrected for ZPE based on the B3LYP-DFT values. [c] Corrected for BSSE.

31G** calculations on all of the B3LYP-DFT geometries. For some of the structures, the DIIS algorithm converges to an unstable wave function in the SCF calculations; using the Quadratic Convergence (QC) method eliminates this problem. The underlying UHF wave functions suffer more from spin contamination than the DFT wave functions (see Table 2). Even after annihilation of the first spin contaminant, ⟨S**2⟩ remains as high as 0.7538 for the transition states. Concerning the barrier heights, one must be cautious in comparing the values obtained at these levels of theory, also in view of the small energy range. In particular, the basis set used (6-31G**) is fairly small for CCSD(T) calculations, the CC energies are calculated for DFT-optimized geometries, and the UHF wave function suffers from spin contamination. The CC barrier heights are therefore unreliable, because of the difference in bonding in the minima and the transition states. Still, at this level of theory the relative energies within the group of minima, and the relative energies within the group of transition states should be comparable to the DFT results. The largest differences in relative energies are found for the H-bonded geometries, where the largest influence of basis set size and geometry can be expected.

The relative energy for the hydroxyethoxy dissociation products needs to be corrected for basis set superposition error (BSSE). As argued by Van Duijneveldt et al.,[14] this is correctly estimated using the Boys−Bernardi counterpoise procedure,[15] in which the energy of each fragment is calculated at the geometry it has in the parent molecule, both with and without the presence of the ghost orbitals of the other fragment. The GAUSSIAN 94 program suite[16] was used for all quantum chemical computations.

Quantum Chemical Results

Unless stated otherwise, all data mentioned below are those obtained at the B3LYP-DFT/6-31G** level of theory. Table 1 lists the ZPE-corrected relative energies for all rotamers of the hydroxyethylperoxy and hydroxyethoxy radicals, as well as for all rotamers of the transition state for C−C bond rupture in the hydroxyethoxy radicals. The only coordinates given in Table 1 are the dihedral angles O−C−C−O, H−O−C−C, and C−C−O−O (where applicable), since they serve to define the different rotamers. The complete geometric specifications can be found in the Supporting Information. Figure 1 shows some of the rotamers; a three-dimensional representation of the complete set of structures is included in the Supporting Information. Also included there is a listing of the vibrational wavenumbers for all molecules discussed here.

For the two radicals, each of the dihedral angles mentioned above has three values corresponding to a minumum in energy. As such, there are 27 (=3 × 3 × 3) distinct $HO-CH_2-CH_2-OO$ internal-rotation conformers possible and 9 (=3 × 3) $HO-CH_2-CH_2O$ rotamers. These can be paired (by inverting the sign of all dihedral angles) in enantiomers with the same energy, except the structures with C_s symmetry which are their own mirror image. The transition states for C−C bond rupture in the hydroxyethoxy radical have near-planar CH_2OH moieties. As a result, only two values for the H−O−C−C dihedral angle correspond to a local minimum in energy, leading to 6 (=3 × 2) $HOCH_2-CH_2O$ transition state conformers, i.e., three pairs of enantiomers.

The relative energies of the different internal-rotation conformers are determined by steric hindrance, Coulomb attraction and repulsion between the partially charged atoms, and (where geometrically possible) by hydrogen bonding between the hydroxy H and an oxygen of the (per)oxy function. Three of the thirteen energetically different $HOCH_2CH_2OO$ rotamers characterized are stabilized by hydrogen bonding: the distance between the hydroxy H and the outer peroxy O in the most

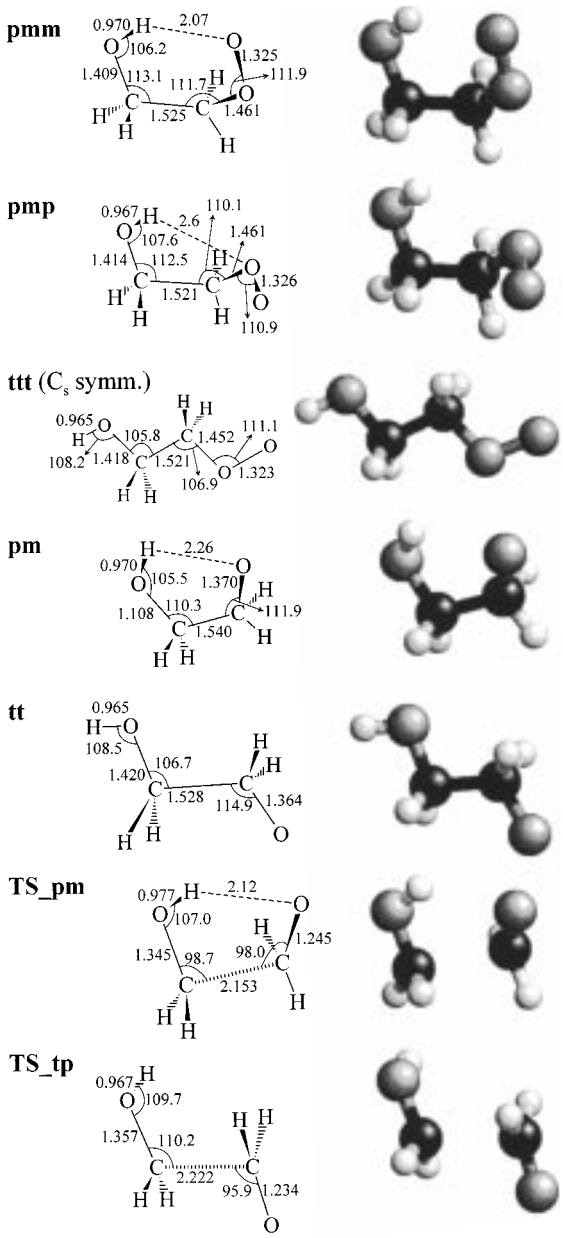

Figure 1. Selected geometric parameters for rotamers of the $HOCH_2CH_2OO$ radicals, the $HOCH_2CH_2O$ radicals, and the transition states for C−C bond rupture in the $HOCH_2CH_2O$ radicals. Bond lengths are in Ångstroms, angles in degrees.

stable rotamer is 2.07 Å; the next two most stable structures, with relative energies of 1.1 and 1.8 kcal/mol, have a weaker hydrogen bond with the inner peroxy oxygen, with H···O distances of 2.6 and 2.5 Å, respectively. These conformers all have the hydroxy H pointing directly toward the peroxy group but have different orientations of the terminal peroxy-oxygen. All other structures have H···O distances above 3.3 Å, precluding stabilization by hydrogen bonding, and the relative energies of these rotamers are at least 2.7 kcal/mol above the lowest structure. One rotameric geometry and its enantiomer were found to be unstable toward internal rotation of the hydroxy H; they convert without a barrier to the most stable rotamer (pmm).

The $HOCH_2CH_2O$ radical (further referred to as the oxy radical) has five energetically different rotamers, of which one has a hydrogen bond, with an H···O distance of 2.26 Å; the amount of stabilization is comparable to that of the hydrogen-bonded peroxy radicals. Also analogous to the peroxy radicals, the non-H-bonded $HOCH_2CH_2O$ rotamers have H···O distances above 3.4 Å, with relative energies at least 1.8 kcal/mol above the most stable structure. Using the calculated relative energies, vibrational frequencies and rotational constants of all structures, it is found for both radicals that the hydrogen-bond-stabilized rotamers should account for about 95% of the thermal equilibrium population at 290 K. The differences in relative energies for the DFT and CC quantum chemical methods are very small (average: ±0.2 kcal/mol), indicating that the DFT geometries and energies are good estimates and that B3LYP-DFT reliably describes the rotamerism.

Besides the relative energy, other observations support the intramolecular hydrogen bonding. Characteristic for hydrogen bonds is the frequency shift for the OH stretch vibration. This frequency is around 3650 to 3690 cm^{-1} for the non-H-bonded rotamers, while the most stable H-bonded geometries have frequencies of approximately 3615 cm^{-1}, a shift of 40−80 cm^{-1}. As a reference, in β-hydroxyketones[5] the OH-stretch frequency decreases down to approximately 3520 cm^{-1}, from around 3650 cm^{-1} in normal alcohols. The hydrogen bond also increases the rigidity of the structure, exemplified by the higher values for the smallest wavenumbers, which correspond to vibrational modes affecting the entire molecule. In particular, the frequencies for the internal rotation around and for wagging across the C−C bond are systematically higher for the H-bonded rotamers compared to the other rotamers. The same effect can be observed for the wavenumber for internal rotation of the hydroxy H.

The experimental energy barrier for the thermal decomposition of $HOCH_2CH_2O$, reaction 6, is only 10−11 kcal/mol,[1] derived at temperatures near ambient. Under these conditions, the bulk of the thermalized hydroxyethoxy radicals are present as H-bonded rotamers. Given this stabilization by hydrogen bonding, the measured barrier is surprisingly low for a dissociation where one expects the breaking of both a C−C bond and a hydrogen bond. Also, it deviates significantly from the Arrhenius activation energy proposed recently by Atkinson[17] (14.5 kcal/mol). As shown below, the low energy barrier to dissociation can be traced back to the persistence of the intramolecular hydrogen bond throughout the C−C bond rupture. Three structurally and energetically different transition states, each with an enantiomeric partner, were characterized. The lowest-lying TS is an H-bonded rotamer with a relative energy 9.9 kcal/mol above its parent, the H-bond stabilized lowest-energy oxy radical. This barrier is in close accord with the experimental value of 10−11 kcal/mol. Despite the C−C bond length of 2.15 Å, we find a H···O distance in this transition state of only 2.12 Å, even slightly smaller than in its oxy radical parent. This is possible only because both the CH_2OH and CH_2O moieties become almost planar while the C−C bond elongates, such that the distance between the hydroxy H and the oxy O remains almost unchanged up to and even beyond the TS. The other two transition states, with H···O distances larger than 3.8 Å, have relative energies 1.9 and 3.3 kcal/mol above this lowest decomposition TS, clearly marking the stabilizing effect of the hydrogen bond. There are indications that the H-bond in the TS is slightly stronger than in the parent radical: the H···O distance is even shorter, and the reduction of the hydroxyl O−H stretch frequency (by 170 cm^{-1}) is more pronounced; moreover, the frequencies of the (hindered) internal rotations about the C−C axis and of the hydroxy H about the O−*C* axis differ more strongly from the values of the non-H-bonded structures (see Supporting Information). However, the energy data indicate that the H-bond stabilization remains nearly unchanged (see

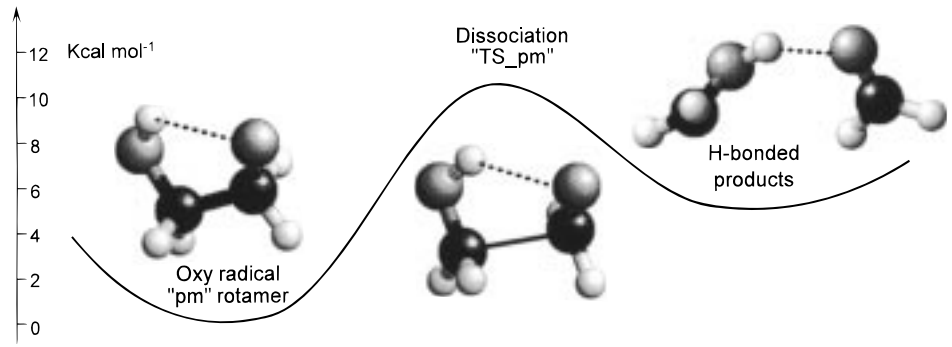

Figure 2. Schematic potential energy diagram of the dissociation pathway of the H-bonded $HOCH_2CH_2O$ radical. The product is an H-bonded $CH_2OH\cdots OCH_2$ complex that in turn can dissociate to $CH_2OH + CH_2O$.

Table 1): the energy difference between the H-bonded TS (TS_pm) and the H-bonded oxy radical (pm) of 9.9 kcal/mol is almost identical to the difference between the lowest non-H-bonded TS (TS_tp) and the lowest non-H-bonded oxy radicals (tt and tp). It should be emphasized that the H-bonded oxy rotamers as well as the H-bonded TS constitute about 95% of the respective thermal populations at 290 K, and therefore account for the bulk of the reactive flux in the thermal decomposition of the $HOCH_2CH_2O$ radical. The remarkable persistence of the H-bond in the lowest transition state results in a lower-energy dissociation path for the H-bonded rotamers than would exist if no H-bonding were possible in the TS.

Figure 2 represents a schematic potential energy diagram of this dissociation path. The product is an H-bonded $CH_2OH\cdots OCH_2$ complex with a relative energy of 5 kcal/mol with respect to the oxy rotamer parent; subsequent breaking of the H-bond and decomposition to $CH_2OH + CH_2O$ occurs through a very loose TS, faces a barrier of only a few kcal/mol, and will therefore be very fast. The relative energy for the separated products, as listed in Tables 1 and 2, is corrected for BSSE; this correction was 2.7 kcal/mol at the DFT level of theory, and 3.2 kcal/mol for the CC calculations. The strength of the hydrogen bond between the H-bonded products is then about 3 kcal/mol. The relative energy of the products with respect to the most stable H-bonded oxy radical is 8.2 kcal/mol at the DFT level of theory, and 6.8 kcal/mol at the CC level. The results are close to the value of 9 ± 3 kcal/mol obtained from the 0 K experimental data for CH_2OH and CH_2O,[18,19] and a thermochemical estimate for $\Delta H^\circ_{0f}(HOCH_2CH_2O) \approx [\Delta H^\circ_{0f}(CH_3CH_2O) + \Delta H^\circ_{0f}(HOCH_2CH_3) - \Delta H^\circ_{0f}(CH_3CH_3)]$[19,20] $+ \Delta H_{st}$(H-bond), with the latter the H-bond stabilization energy of 2 kcal/mol in hydroxyethoxy.

The Coupled Cluster barrier heights for decomposition of the oxy rotamers (about 14 kcal/mol) are markedly higher than the DFT results and the experimental value. As shown later, such barrier heights are irreconcilable with the experimentally observed product distribution.[1] These higher barrier heights are probably an artifact of the small basis set used, the single point approach, and the spin contamination (see higher). Sample single point calculations using a slightly larger basis set (6-311++G**) already reduce the lowest barrier to 12.4 kcal/mol, showing the sensitivity of the absolute barrier height to the CC basis set size. Improving the energies for all geometries further would require CC geometry optimizations with even larger basis sets, a daunting task at the current level of technology and beyond the scope of this work. The energy spacing between the different TS rotamers is comparable to those found at the DFT level, indicating that the rotamerism and hydrogen bonding have comparable effects at both levels of theory.

We also calculated some transition states for internal rotation in the oxy radical. As expected, these were approximately 0.5−1.5 kcal/mol above the highest of the two pertaining minima. We did not pursue this matter any further, since these barrier heights indicate that internal rotation occurs much more rapidly than dissociation at all reaction conditions, ensuring fast (microcanonical) equilibration in atmospheric conditions.

Finally, we also examined the possibility of intramolecular hydrogen transfer in the hydroxyethylperoxy radicals from the OH group to the radicalar oxygen, aided by the H-bond. The most stable hydroperoxyethoxy radical rotamer, with a hydrogen bond comparable to the most stable hydroxyethylperoxy rotamer, has a relative energy of about 19 kcal/mol above the latter (see Supporting Information). Since 1,5-H shifts involve almost no strain,[18] the strongly exothermal reverse reaction of OCH_2CH_2OOH faces a barrier of only a few kcal/mol and should therefore be much faster than both the competing reaction with O_2[18] and the thermal dissociation to CH_2O and CH_2OOH, which is expected to be endoergic for 16 ± 4 kcal/mol, based on a BAC-MP4 $\Delta H^\circ_{0f}(CH_2OOH)$ value[20] and on a $\Delta H^\circ_{0f}(HOCH_2CH_2O_2)$ estimate obtained in a similar way as that for the oxy radical. As a result, the isomerization should tend to an equilibrium, with a negligible fraction of the radicals reacting as OCH_2CH_2OOH. Also, prompt isomerization and dissociation to $CH_2O + CH_2OOH$ of the still activated nascent $HOCH_2CH_2O_2^\dagger$ radicals formed in reaction 2 is unlikely to be of importance. The total energy required, at least 35 ± 4 kcal/mol, is only slightly less than the ≈39 kcal/mol internal energy content of the peroxy† radical, composed of the $R-O_2$ bond energy of 34 kcal/mol[4] plus some 3 kcal/mol average thermal internal energy in the entrance TS of reaction 2, plus the H-bond stabilization of the hydroxyethylperoxy radical of 2 kcal/mol. Even if the required energy is overestimated by 5 kcal/mol, the effective rate of the above process, according to an RRKM estimate, would still be only 3×10^7 s^{-1}, and therefore far below the rate of collisional deactivation in atmospheric conditions. Likewise, the microcanonical equilibrium fraction of activated $OCH_2CH_2OOH^\dagger$, about 10^{-3}, is far too small for the reaction thereof with O_2 to compete effectively with collisional deactivation of $HOCH_2CH_2O_2^\dagger$, even if the reaction with O_2 is fast.

The good accord obtained above between the DFT and CC relative energies for the hydroxyeth(ylper)oxy minima, between the DFT relative energies for the oxy decomposition transition states and the experimental barrier heights, and between the calculated and observed product distributions (see further) indicates that the B3LYP-DFT optimized structures, energies and vibrational frequencies adequately describe the rotamerism in hydroxyalkyl(per)oxy radicals and the effects of the intramolecular hydrogen bonding that we highlighted in these molecules.

Kinetics of Prompt and Thermal Decomposition of Hydroxy−Ethoxy Radicals

In laboratory studies, it has been shown that in atmospheric conditions (1 atm, 298 K, NO present) 80% of the hydroxyethoxy radicals formed in reaction 2 decompose to $CH_2OH + CH_2O$, rather than reacting with O_2.[1−3] Here, we will show the importance of the persistence of the intramolecular hydrogen bond during the oxy radical decomposition in theoretically explaining this experimental result. The theoretical kinetic analysis described below was performed using our URESAM computer program suite.[21]

As shown above, the stabilization afforded by the H-bond is nearly the same in the hydroxyethylperoxy and -oxy radicals; hence, one can adopt an exoergicity for reaction 3 equal to that for the analogous reaction of the unsubstituted ethylperoxy radical, i.e., 11 kcal/mol.[4] Assuming a relative energy of the peroxynitrite intermediate with respect to the reactants as for the 1-butyl analogue,[14] and using B3LYP-DFT frequencies for $HOCH_2CH_2OONO$ and estimated vibrational frequencies for the variational entrance and exit transition states, we obtain an RRKM lifetime for the activated peroxynitrite of 5×10^{-12} s. This is sufficiently long to ensure ergodicity and even equilibrium among all the different rotamers. On the other hand, this lifetime is too short for significant collisional energy loss in atmospheric conditions, such that the internal-energy distribution of the peroxynitrite at dissociation is nearly equal to that at formation, $F_{form}(E_{th})$, which can be obtained from the sum of states function for the entrance TS.[22] The dissociation of an alkylperoxynitrite to an oxy radical + NO_2 occurs through a barrierless exit channel,[14] implying a late and loose transition state. The nascent vibrational energy distribution for the resulting $HOCH_2CH_2O$ fragment can then be obtained according to the Separate Statistical Ensemble (SSE) theory of Wittig et al.[23] by assuming a statistical distribution of the available internal energy E_{tot} over the vibrational degrees of freedom of each of the two fragments and over the degrees of freedom for their relative motion. Such distribution amounts to equal probabilities for all "internal" quantum states of the separating products with given total energy E_{tot} and is determined by the energy-dependent densities of states for these three sets of degrees of freedom. The six modes of relative rotation and translation are treated as unhindered free particle motions with combined state density therefore varying as $E^{6/2-1}$. While the basic rationalization for applying the SSE theory to this type of problem has already been outlined in the complementary paper,[1] its implementation for the specific case at hand is detailed below. To account for the formation of the different oxy rotamers, we must extend the SSE theory (fully consistent with its philosophy) by considering the simultaneous formation of all conformers, weighted according to their densities of states and taking into account their relative energies. For a given energy available to the products, E_{tot}, the probability P_{A_i} of forming an oxy radical in rotameric form i with internal energy E_A is given by

$$P_{A_i}^{E_{tot}}(E_A) = \frac{N_{A_i}(E_A)\int_0^{E-E_A}[N_{NO_2}(E_{NO_2})\,N_{rel.mot.}(E_{tot}-E_A-E_{NO_2})]\,dE_{NO_2}}{\int_0^{E_{tot}}\{(\sum_i N_{A_i}(E_A))\int_0^{E-E_A}[N_{NO_2}(E_{NO_2})\,N_{rel.mot.}(E_{tot}-E_A-E_{NO_2})]\,dE_{NO_2}\}\,dE_A}$$

Here, $N(E)$ is the density of states for the considered fragment or for the relative motion of the fragments and E_A is the energy above the ground state *of the most stable rotamer*. The energy distribution for NO_2 and for relative motion of the fragments is described by similar equations. A closer inspection reveals that the partitioning of E_{tot} over the two fragments and the degrees of freedom of their relative motion is not determined by the absolute values of the respective densities of states but rather by the functional dependences on energy thereof; the set of degrees of freedom with combined density of states showing the steepest energy dependence will be the most favored. The energy E_{tot} available to the products comprises the exoergicity $-\Delta E_3$ of reaction 3 and the internal thermal energy of the (variational) entrance transition state, with distribution $F_{form}(E_{th})$. In principle, the internal energy should be corrected for the change in rotational energy E_{rot} between the exit and entrance transition states in accordance with the respective moments of inertia, as imposed by the conservation of angular momentum. Any decrease of E_{rot} would be forced into additional internal energy. However, the initial E_{rot} of $(3/2)kT$ is small at room temperature;[23] furthermore, its relative change should be small since both variational transition states are nearly equally loose. The correction is therefore expected to amount to at most about kT or ≈0.6 kcal/mol at 300 K and can be neglected with respect to the sum of $-\Delta E_3 = 11$ kcal/mol plus $\langle E_{th}\rangle \approx 4$ kcal/mol.

To obtain the probability $P_i(E_A)$ of formation of an oxy rotamer i with vibrational energy E_A, the equation above has to be integrated over the energy distribution of E_{tot}. Finally, summing over all rotamers gives the probability of formation of oxy radicals with energy E_A. The equations can readily be adapted for an energy-grained description. The results of this analysis are already described in the complementary article.[1]

The $HOCH_2CH_2O$ radicals formed in reaction 3 will either decompose promptly or assume a thermal energy distribution by collisional energy transfer with bath gas molecules. The relative importance of reactions 4 and 5 was quantified by Master Equation analysis[22] using the $P_i(E_A)$ as input. Dissociation rate constants were obtained using RRKM theory,[23] based on the DFT relative energies and vibrational characteristics. Troe's biexponential model[24] was used to calculate the collisional energy transfer probabilities, with an average energy transfer $\langle\Delta E_{overall}\rangle$ of -100 cm^{-1} per collision.[25] The effects of isomerization by internal rotation prior to dissociation were modeled by including transition states interconnecting all minima. We used the DFT vibrational frequencies of the transition states for internal rotations but set the barrier heights at 5.5 kcal/mol above the lowest rotamer, an estimated upper limit. Even with this barrier height, all internal rotations are at least 2 orders of magnitude faster than dissociation, ensuring equilibrium between all rotamers at each considered excess energy. Radicals with an internal energy below the isomerization barrier are assumed to be stabilized and are collected in a sink.[22] Thermal reactivation occurs on a much slower time scale ($k_{therm} \sim 10^5$ s^{-1}, see below) than prompt dissociation ($k_{diss} \sim 10^8-10^9$ s^{-1}), supporting the use of a sink to separate "prompt" from "thermal" dissociation; the results obtained are not sensitive to the exact cutoff energy adopted. Results of the Master Equation analysis for this reaction were reported earlier;[1] thus, we predict an average of 29% prompt dissociation for $T = 225-300$ K and 1 atm air for a decomposition barrier height of 10 kcal/mol, in good accord with the experimental value of $25 \pm 6\%$.[1] Table 3 summarizes the sensitivity of this result to a number of parameters. In the complementary article,[1] results obtained when using a barrier height of 11 kcal/mol were already reported. Of particular interest here is the result with an assumed barrier height of 13 kcal/mol, which leads to less than 4% prompt dissociation at 300 K. This barrier height reflects a hypothetical

TABLE 3: Results of the Master Equation Calculations on Prompt Dissociation of β-Hydroxyethoxy Radicals Formed in the RO_2 + NO Reaction, for Several Combinations of Reaction Parameters

parameter varied	value used[a]	prompt dissociation fraction (%)
Barrier height for dissociation	**10**	37.7
(kcal/mol)	11	21.5
	13	3.7
Exoergicity of the RO_2 +	**11**	37.7
NO reaction (kcal/mol)	13	57.2
pressure (atm)	0.5	42.1
	1.0	37.7
	1.5	34.0
temp (K)	**300**	37.7
	250	25.7
	200	18.4
temp (K) and pressure (atm)	220, 0.2[b]	29.9

[a] Numbers in bold are the default values for the parameter. [b] Reaction conditions at the top of the troposphere (altitude 15 km).

case where the oxy radicals will quickly isomerize to the H-bonded rotamers, as is the case above, but no H-bond stabilization could occur in the transition states, such that the lowest dissociation TS would have a relative energy comparable to TS_pp and TS_tp.

The rate of the thermal dissociation of the hydroxyethoxy radicals, reaction 6, can be estimated using Transition State theory (TST) and Troe's low-pressure theory,[26] yielding respectively the high- and low-pressure limits, from which the rate constant at a specific pressure is then derived using Troe's fall-off formalism.[27] As made clear above, for thermal dissociation at 298 K only the dissociation channel through the lowest transition state has to be considered. The TST expression for the high-pressure rate coefficient is

$$k_\infty = \frac{kT}{h}\frac{Q^\ddagger}{Q}e^{-E_0/RT} = A_\infty e^{-E_0/RT}$$

On the basis of the vibrational and rotational characteristics of the lowest-energy oxy radical and lowest-energy decomposition TS, obtained in the quantum chemical DFT study, we calculate a partition function ratio $Q^\ddagger/Q$ at 298 K of 1.80 and hence a pre-exponential factor $A_\infty = 1.1 \times 10^{13}$ s^{-1}. Adopting the DFT barrier height E_0 of 10 kcal/mol leads to a high-pressure rate coefficient at 298 K of $k_\infty = 5.1 \times 10^5$ s^{-1}. As already indicated in the Computational Details section, e.g., for the isopropoxy decomposition, TST calculations based on the DFT rovibrational data generally compare well with the experimental data.

The low-pressure limit is calculated using the Troe equation[27]:

$$k_0 = kTZ_{LJ}[M]\beta\frac{N(E_0)\,e^{-E_0/kT}}{Q_{vib}}F_E F_{anh}F_{rot}F_{int.rot.}$$

with the Lennard-Jones collision frequency $Z_{LJ} = 3.7 \times 10^{-10}$ s^{-1} at 298 K for N_2 as bathgas M, using $\epsilon_{A-A} = 391$ K and $\sigma_A = 4.5$ Å. The adopted $\langle\Delta E_{tot}\rangle$ of -100 cm^{-1} results in a collision efficiency $\beta = 0.25$. The (harmonic) vibrational density of states $N(E_0)$ for the lowest oxy rotamer at an excess energy equal to the barrier height $E_0 = 10$ kcal mol^{-1} is 6.87×10^3 states per kcal/mol, as obtained using the exact count algorithm of Stein−Rabinovitch;[27] the harmonic vibrational partition function is $Q_{vib} = 3.00$. Using Troe's formulas, the correction factor F_E for the energy dependence of the density of states is estimated at 1.35, while correction for the anharmonicity is close to unity for this case: $F_{anh} = 1.10$. The effect of overall rotation can be estimated from the moments of inertia of the DFT-optimized geometries, leading to $F_{rot} = 2.07$. The contribution of the two hindered internal rotors is more difficult to assess; given the relatively high barriers for internal rotation, especially for the most stable rotamer, we treat each rotor as an oscillator with an estimated individual anharmonicity contribution of a factor 1.75,[27] leading to a total correction factor $F_{int.rot} \approx 3.0$. Given the particle density [M] of 2.45×10^{19} molecules/cm^3 at 1 atm and 298 K, the low-pressure first-order rate constant becomes $k_0 = 1.35 \times 10^6$ s^{-1}. On the basis of k_∞, k_0, and an estimated broadening factor F_{cent} of 0.5, we finally obtain a rate constant at a pressure of 1 atm of $k_{6,atm} = 2.1 \times 10^5$ s^{-1}, still a factor 2.5 below the high-pressure limit. This result compares favorably to the thermal rate constant derived from experimental data:[1] $k_{6,exp} = 1.3 \times 10^5$ s^{-1} within a factor of 2. In contrast, repeating the calculation for a barrier height of 13 kcal/mol yields a thermal rate constant of only 2×10^3 s^{-1}, about 65 times lower than the experimental value.

From this, it is straightforward to predict the total yield of $CH_2OH + CH_2O$ in the OH-initiated oxidation of ethene at 298 K and 1 atm air. Assuming that the rate constant for the $HOC_2H_4O + O_2$ reaction is equal to that for $C_2H_5O + O_2$, i.e., $k_7 = 6 \times 10^{-14} \exp(-550/T)$ cm^3 molecule^{-1} s^{-1},[28] we find a pseudo-first-order rate constant at 298 K and 0.2 atm partial pressure O_2 of $k_7 = 5 \times 10^4$ s^{-1}; i.e., reaction with O_2 is 4.1 times slower than thermal dissociation. From the prompt dissociation fraction of 38% at 298 K and the ratio of the thermal rate constants $k_6/(k_6 + k_7)$, it follows that 88% of the hydroxyethoxy radicals dissociate to $CH_2OH + CH_2O$. This result is directly comparable to the experimental value of 80%. The theoretical prediction for a barrier height of 13 kcal/mol is about 5% dissociation. Confrontation of the predictions with the experiment clearly shows that the persistence of hydrogen bonding is an essential element in describing the dissociation of β-hydroxyethoxy radicals.

Conclusions

We have theoretically identified intramolecular hydrogen bonds in β-hydroxyethylperoxy and β-hydroxyethoxy radicals, using the B3LYP-DFT/6-31G** level of theory. The stabilization energies found are 1.5−2.5 kcal/mol, typical values for such H-bonds. In atmospheric conditions, both types of radicals are present dominantly as the stabilized rotamers. The H-bond found in the most stable structures is conserved during the C−C bond rupture in $HOCH_2-CH_2O$. The unexpected persistence of the H-bond in the decomposition TS provides a low-energy pathway for dissociation of the H-bond stabilized hydroxyethoxy radicals, leading to an energy barrier for dissociation of ≈10 kcal/mol. This theoretical barrier height compares favorably with the activation energy derived from recent experimental measurements, described in a complementary paper.[1]

Based primarily on the results of the DFT characterization, detailed statistical and kinetics calculations were performed to model final product formation in the OH-initiated atmospheric oxidation of ethene in the presence of NO. These calculations reproduce the experimental results independently. First, the nascent vibrational energy distribution of the hydroxyethoxy radicals was calculated, taking into account the chemical activation effects of the hydroxyethylperoxy + NO reaction and the statistical distribution of the available energy over the hydroxyethoxy and NO_2 products and over the degrees of freedom for their relative motion; thereby, the relative contribution of all different rotameric forms of the oxy radical was evaluated. The ratio of prompt dissociation to collisional

stabilization of the activated oxy radicals was quantified in a subsequent Master Equation analysis, incorporating the effects of fast isomerization of the different oxy rotamers and allowing for dissociation through all transition state rotamers. It was found that at 298 K and 1 atm 38% of the ethoxy radicals dissociate promptly, in fair accord with the experimental result of 26%.[1] The rate constant for thermal dissociation of hydroxyethoxy radicals was estimated using TST theory and Troe's low-pressure and falloff theories. Again, the predicted rate constant, $k_{1atm} = 2.1 \times 10^5\ s^{-1}$ at 298 K, compares favorably with the result derived from experimental data,[1] $1.3 \times 10^5\ s^{-1}$. We predict a total yield of 88% $CH_2OH + CH_2O$ in the tropospheric oxidation of ethene, directly comparable to the experimentally observed 80%. All kinetic calculations were repeated for a hypothetical case where the hydrogen bond is broken in the TS for dissocation, with a barrier estimated at 13 kcal/mol. The dissociation of hydroxyethoxy radicals is then outrun by the reaction with O_2, giving a total yield of only about 5% $CH_2OH + CH_2O$. The qualitative difference between the latter result and the experimental values stresses the importance of the persistence of the intramolecular hydrogen bond while the hydroxyethoxy radical dissociates in explaining the observed product distribution. From a chemical viewpoint, the persistence of the weak hydrogen bond while the much stronger C−C bond ruptures is noteworthy. It is consequenced by two simultaneous structural changes: (i) the C−C bond elongates, and (ii) the CH_2O and CH_2OH moieties become nearly planar, such that during the critical phases of the dissociation, only the carbon atoms move appreciably.

Acknowledgment. This work was financially supported by the European Commission, the Flemish Community, and the *Fonds voor Wetenschappelijk Onderzoek*, Flanders. Thanks are due to Dr. Jamal El Yazal for his help in the ab initio calculations.

Supporting Information Available: Geometric coordinates, figures containing three-dimensional model representations, moments of inertia, and vibrational wavenumbers for all hydroxyeth(ylper)oxy rotamers, dissociation transition states, and products, for the most stable hydroperoxyethoxy radical rotamer, and for the ethoxy and isopropoxy dissocation. This information is available free of charge via the Internet at http://pubs.acs.org.

References and Notes

(1) Orlando, J. J.; Tyndall, G. S.; Bilde, M.; Ferronato, C.; Wallington, T. J.; Vereecken, L.; Peeters, J. *J. Phys. Chem. A* **1998**, *102*, 8116.

(2) Niki, H.; Maker, P. D.; Savage, C. M.; Breitenbach, L. P. *J. Phys. Chem.* **1978**, *82*, 135.

(3) Barnes, I.; Becker, K. H.; Ruppert, L. *Chem. Phys. Lett.* **1993**, *203*, 295.

(4) Lightfoot, P. D.; Cox, R. A.; Crowley, J. N.; Destiau, M.; Hayman, G. D.; Jenkin, M. E.; Moortgat, G. K.; Zabel, F. *Atmos. Environ.* **1992**, *26A*, 1805.

(5) Diallo, A. O. *Spectrochim. Acta* **1972**, *28A*, 1765. Pitzner, L. T.; Atalla, R. H. *Spectrochim. Acta* **1975**, *31A*, 911.

(6) Becke, A. D. *J. Chem. Phys.* **1992**, *96*, 2115; ibid. **1992**, *97*, 9173; **1993**, *98*, 5648.

(7) Lee, C.; Yang, W.; Parr, R. G. *Phys. Rev. B* **1988**, *37*, 785.

(8) Scott, A. P.; Radom, L. *J. Phys. Chem.* **1996**, *100*, 16502.

(9) Vereecken, L.; Pierloot, K.; Peeters, J. *J. Chem. Phys.* **1998**, *108*, 1068.

(10) Hobza, P.; Sponer, J.; Reschel, T. *J. Comput. Chem.* **1995**, *16*, 1315.

(11) Somnitz, H.; Zellner, R. To be published.

(12) Batt, L.; Milne, R. T. *Int. J. Chem. Kinet.* **1977**, *9*, 549.

(13) Devolder, P.; Fittschen, C.; Frenzel, A.; Hippler, H.; Poskrebyschev, G.; Striebel, F.; Viskolcz, B. Complete falloff curves for the unimolecular decomposition of i-propoxy radicals between 332 and 410 K. *Phys. Chem.—Chem. Phys.*, to be submitted.

(14) Jungkamp, T. P. W.; Smith, J. N.; Seinfeld, J. H. *J. Phys. Chem. A* **1997**, *101*, 4392.

(15) Van Duijneveldt, F. B.; Van Duijneveldt-van de Rijdt, C. M.; Van Lenthe, J. H. *Chem. Rev.* **1994**, *94*, 1873.

(16) Boys, S. F.; Bernardi, F. *Mol. Phys.* **1970**, *19*, 553.

(17) Frisch, M. J.; Trucks, G. W.; Schlegel, H. B.; Gill, P. M. W.; Johnson, B. G.; Robb, M. A.; Cheeseman, J. R.; Keith, T.; Petersson, G. A.; Montgomery, J. A.; Raghavachari, K.; Al-Laham, M. A.; Zakrzewski, V. G.; Ortiz, J. V.; Foresman, J. B.; Cioslowski, J.; Stefanov, B. B.; Nanayakkara, A.; Challacombe, M.; Peng, C. Y.; Ayala, P. Y.; Chen, W.; Wong, M. W.; Andres, J. L.; Replogle, E. S.; Gomperts, R.; Martin, R. L.; Fox, D. J.; Binkley, J. S.; Defrees, D. J.; Baker, J.; Stewart, J. P.; Head-Gordon, M.; Gonzalez, C.; Pople, J. A. *Gaussian 94*, Revision E.2; Gaussian, Inc.: Pittsburgh, PA, 1995.

(18) Atkinson, R. *Int. J. Chem. Kinet.* **1997**, *29*, 99.

(19) Atkinson, R. *J. Phys. Chem. Ref. Data* **1997**, *26*, 215.

(20) Lias, S. G.; Bartmess, J. E.; Liebman, J. F.; Holmes, J. L.; Levin, R. D.; Mallard, W. G. *J. Phys. Chem. Ref. Data* **1998**, *17*, 1.

(21) Melius, C. F. BAC-MP4 Heats of Formation and Free Energies. Sandia National Laboratories, 1996.

(22) Vereecken, L.; Huyberechts, G.; Peeters, J. *J. Chem. Phys.* **1997**, *106*, 6564.

(23) Forst, W. *Theory of Unimolecular Reactions*; Academic Press: New York, 1973.

(24) Wittig, C.; Nadler, I.; Reisler, H.; Noble, M.; Catanzarite, J.; Radhakrishnan, G. *J. Chem. Phys.* **1985**, *83*, 5581.

(25) Troe, J. *J. Chem. Phys.* **1977**, *66*, 4745.

(26) Oref, I.; Tardy, D. C. *Chem. Rev.* **1990**, *90*, 1407.

(27) Troe, J. *J. Chem. Phys.* **1977**, *66*, 4758; **1979**, *83*, 114.

(28) Stein, S. E.; Rabinovitch, B. S. *J. Phys. Chem.* **1973**, *58*, 2438.

(29) DeMore, W. B.; Sander, S. P.; Golden, D. M.; Hampson, R. F.; Kurylo, M. J.; Howard, C. J.; Ravishankara, A. R.; Kolb, C. E.; Molina, M. J. Chemical kinetics and photochemical data for use in stratospheric modeling; evaluation number 12. NASA JPL Publ. No. 97-4, 1997.